



Article

Multifunctional Nanocrystalline Cu–Ti Thin Films Enhance Survival and Induce Proliferation of Mouse Fibroblasts In Vitro

Małgorzata Osełkowska ¹, Damian Wojcieszak ² , Danuta Kaczmarek ², Michał Mazur ² , Agata Obstarczyk ²  and Bogumiła Szponar ^{1,*} 

¹ Hirszfeld Institute of Immunology and Experimental Therapy, Polish Academy of Sciences, Weigla 12, 53-114 Wrocław, Poland; osekowska.malgorzata@gmail.com

² Faculty of Microsystem Electronics and Photonics, Wrocław University of Science and Technology, Janiszewskiego 11/17, 50-372 Wrocław, Poland; damian.wojcieszak@pwr.edu.pl (D.W.); danuta.kaczmarek@pwr.edu.pl (D.K.); michal.mazur@pwr.edu.pl (M.M.); agata.obstarczyk@pwr.edu.pl (A.O.)

* Correspondence: bogumila.szponar@hirszfeld.pl

Abstract: This paper describes the effect of a nanocrystalline thin film based on copper and titanium on mouse fibroblast cells. Cu–Ti coatings were prepared using magnetron sputtering. In their composition was 25 at.% Cu and 75 at.% Ti. The goal of the study was to evaluate the effect of the material on the survival, migration, and proliferative capabilities of mouse L929 fibroblasts. The Cu₂₅Ti₇₅ material had no effect on the induction of cell death and did not disturb the cell cycle phase. The study showed a unique effect of a Cu₂₅Ti₇₅ thin film on mouse fibroblast cells, and the results concerning mitochondrial activity, cell proliferation, and migration proved that the material is nontoxic and shows proliferative properties in a wound healing test. The possible biomedical applications of the new nanocrystalline thin film biomaterial with multifunctional properties are described.

Keywords: multifunctional coatings; nanocrystalline thin films; copper; titanium; cytotoxicity; cell migration; cell proliferation



Citation: Osełkowska, M.; Wojcieszak, D.; Kaczmarek, D.; Mazur, M.; Obstarczyk, A.; Szponar, B. Multifunctional Nanocrystalline Cu–Ti Thin Films Enhance Survival and Induce Proliferation of Mouse Fibroblasts In Vitro. *Coatings* **2021**, *11*, 300. <https://doi.org/10.3390/coatings11030300>

Academic Editor:
Francesco Di Quarto

Received: 5 February 2021
Accepted: 26 February 2021
Published: 5 March 2021

Publisher's Note: MDPI stays neutral with regard to jurisdictional claims in published maps and institutional affiliations.



Copyright: © 2021 by the authors. Licensee MDPI, Basel, Switzerland. This article is an open access article distributed under the terms and conditions of the Creative Commons Attribution (CC BY) license (<https://creativecommons.org/licenses/by/4.0/>).

1. Introduction

Copper and titanium, as separate components, are well-known and used as biomaterials [1–4]. The properties of Cu–Ti composites have been examined from the mid-twentieth century, and since then, their interactions with microorganisms and the tissues of higher organisms have been investigated extensively.

When the stability of titanium and the high bioactivity of copper are combined, the resulting intermetallic compounds are harder, stiffer, and of lower density and higher resistance to oxidation and abrasion. The main advantage of such a material is its bioactivity, owing to the antimicrobial properties of copper [5,6].

Copper-based materials are a powerful tool against antibiotic-resistant bacteria and nosocomial infections [7–11]. The underlying mechanism involves an intensive migration of copper ions from the material to the environment [12,13]. However, at higher concentrations and under longer exposure, a cytotoxic effect may appear [12,14].

Research on nanocrystalline copper- and titanium-based materials continues towards finding a compound with an optimal ratio of the diverse properties of Cu and Ti that is safe for eukaryotic cells while still significantly reducing the number of microorganisms. We have tested a series of thin nanocrystalline coatings based on copper and titanium in different material compositions [10,15–17]. Recent studies have characterized the physicochemical properties of Cu–Ti thin films with different material compositions [18], as well as the preliminary results concerning their cytotoxicity [15].

The biological consequences for eukaryotic cells that come into direct and/or indirect contact with Cu–Ti nanocrystalline thin films comprise changes to mitochondrial

activity, interruption of the cell cycle, cell death (apoptosis and necrosis), and changes to cell morphology and cell migration abilities. A comprehensive assessment of Cu–Ti films, including an analysis of the physicochemical data and their biological implications, permits the design of biomaterials with the desired cellular and antibacterial response.

We have found that Cu–Ti thin films exhibit antibacterial activity, but their impact on live cells depends on the amount of Cu in their composition [10,15,16]. Cytotoxicity or stimulation of cell growth were observed. In particular, the proliferation and improvement of living cell function following direct or indirect contact with the surface of a nanocrystalline Cu₂₅Ti₇₅ thin film [15] was an interesting observation that motivated us to research the subject further.

This study aimed to determine the nature and strength of the response of mouse fibroblasts exposed to a nanocrystalline Cu₂₅Ti₇₅ thin film with respect to physiochemical properties and antibacterial activity in vitro.

2. Materials and Methods

Thin films based on Cu and Ti in the proportion of 25 at.% to 75 at.% (Cu₂₅Ti₇₅) were prepared using magnetron sputtering [18,19]. The coatings were as deposited during the sputtering of two metallic Ti and one Cu targets in argon plasma. Study [18] presents the method of film preparation in detail. The films were as deposited onto SiO₂ substrates.

10 mm × 10 mm portions of the Cu–Ti thin film applied on both sides of SiO₂ were used for the tests. Energy dispersive spectroscopy (EDS) measurements confirmed the Cu–Ti film composition as 25 at.% Cu and 75 at.% Ti.

2.1. Cell Culture Conditions

Two cell lines, L929 and Balb/C murine fibroblasts, were cultured under constant conditions (5% CO₂, 37 °C, humidity >95%) in a SteriCycle 381 incubator (Thermo Scientific, Waltham, MA, USA). Cell cultures were stored in liquid nitrogen and cultivated in Dulbecco's modified Eagle's medium (DMEM) with 25 mM of HEPES, 4.5 g/L of glucose (Lonza Sales Ltd., Basel, Switzerland), 20% fetal bovine serum (FBS, Lonza Sales Ltd., Basel, Switzerland), and 7% DMSO (Merck, Darmstadt, Germany). To stabilize cell metabolism, two passages were performed using Trypsin–EDTA 0.25% (Merck, Darmstadt, Germany). During cultivation, a DMEM medium with 25 mM of HEPES and 4.5 g/L of glucose was used (Lonza Sales Ltd., Basel, Switzerland) with L-glutamine and 10% FBS (Lonza Sales Ltd., Basel, Switzerland). An automated cell counter (DigitalBio, Seoul, Korea) and a hemocytometer were used to count live cells and spread an appropriate number of cells onto the culture vessels. Cellular response was examined through direct contact of cells with the thin film material and indirectly using material extracts. All procedures were performed under aseptic conditions (MSC Advantage 1.2 laminar chamber Biohazard, Thermo Scientific Waltham, MA, USA).

2.2. Biological Evaluation of a Nanocrystalline Cu₂₅Ti₇₅ Thin Film

The effect of the nanocrystalline Cu₂₅Ti₇₅ thin film on the morphology, metabolic activity, proliferation capacity and migration of murine fibroblasts, the possible interference of the cell cycle phases, and the type of cell death were revealed using L929 cell and mouse fibroblast exposure to the Cu₂₅Ti₇₅ thin film by direct and indirect contact.

2.3. Preparation of Extracts of the Thin Film Material (Indirect Contact)

Thirty pieces of the Cu₂₅Ti₇₅ thin film material (10 mm × 10 mm) were sterilized through exposure to UV light, and 10 mL of the MEM culture medium (Gibco, Waltham, MA, USA) were added to the Cu₂₅Ti₇₅ and incubated in constant, sterile culture conditions for 24 to 240 h (10 days) (SteriCycle 381, Thermo Scientific, Waltham, MA, USA). After incubation, the thin film material was removed and the remaining medium was considered a 100% extract. For each experiment, the appropriate controls were made, i.e., a negative

control (culture medium) and a positive control (1.5 and 4 mg/mL of phenol solution in water, Merck, Darmstadt, Germany).

2.4. Cell Morphology

Cell morphology was recorded using an inverted CKX41 microscope operated on the cellSens Standard imaging software (Olympus, Tokyo, Japan). Direct exposure of the Cu₂₅Ti₇₅ thin films was performed by placing the sample in a sterile culture vessel and incubating with cells for 24 and 72 h. Cell morphology was observed, i.e., cell size, granularity, cell lysis, and reduced cell growth.

2.5. Cytotoxicity of Thin Films Based on Cu and Ti (MTT (3-[4,5-dimethylthiazol-2-yl]-2,5-diphenyl Bromide) Test)

The cytotoxicity of the Cu–Ti thin film was investigated using the L929 and Balb/C murine fibroblast cell lines in indirect contact mode. The level of cytotoxicity for the L929 cell line was measured after 24, 48, and 72 h of indirect exposure to the Cu–Ti thin film. Extract concentrations of 100%, 50%, 25%, and 12.5% were used. L929 cells in the MEM medium were seeded at a density of 1×10^5 /mL per well in a 96-well plate (NUNC, Roskilde, Denmark). After 24 h of cell incubation (with 60% of the culture vessel surface covered with cells), the culture medium was removed and the wells were rinsed with 100 µL of buffered saline (PBS), after which the thin film extracts were applied. A 10% solution of 12 mM MTT (3-[4,5-dimethylthiazol-2-yl]-2,5-diphenyl bromide, Merck, Darmstadt, Germany) in the MEM culture medium was added to each well. After 2 h of incubation, the formazan crystals that formed during the reaction were dissolved with isopropyl acid alcohol (100 µL per well). The suspension was gently mixed and incubated at room temperature for 30 min. Absorbance was read at $\lambda = 570$ nm (Epoch, Biotek Spectrophotometer, Winooski, VT, USA). Cell morphology was documented at each stage of the experiment.

2.6. Clonogenic Test

One hundred mouse fibroblast cells (L929) were placed on six-well plates (NUNC, Roskilde, Denmark). After 8 days of proliferation, the cultures were fixed with 96% ethanol (3 mL/well/5 min) and stained using the May–Grünwald–Giemsa method. A 5% Giemsa dye solution prepared in a Sorensen buffer (2 mL/well/5 min) was used for staining. Colonies were counted using a CKX 41 inverted phase contrast microscope (Olympus, Tokyo, Japan). The result was expressed as the percentage of cell survival in relation to the control.

2.7. In Vitro Scarring Test

Extracts of the thin film material were used in 100% concentrations. L929 fibroblast mouse cells were placed on a sterile 12-well plate (NUNC, Roskilde, Denmark), with 1 mL in each well. After 24 h of proliferation, an identical scratch in the cell monolayer was made with a sterile pipette tip. The speed of cell migration from the edge of the scratch to its center was observed in the presence of material extracts and in direct contact over the next 24 h. Cells not exposed to the extracts were used as a control representing 100% cell migration. Representative microscopic photos were selected at time 0 (immediately after scratching), and 2, 4, 6, and 24 h after scratching. The area of cell migration was monitored over 24 h, and recorded every 3 min using a JuLI Stage (JOS1000, NanoEnTek, Seoul, Korea) mobile recorder and the JuLI Stage inbuilt software (NanoEnTek, Seoul, Korea). The experiment was performed in triplicate.

2.8. Cell Cycle Phase

L929 cells were seeded onto sterile 12-well plates at a density of 1×10^4 cells/mL and incubated. After 24 h, when the culture reached 60% confluence, the culture medium was replaced with extracts from the thin film material and incubated over the next 24 h. Cells were harvested using trypsinisation, centrifuged, and rinsed in PBS twice. Then,

1 mL of 70% frozen ethanol was added to each tube and kept for 30 min at -20°C , after which the cells were centrifuged in PBS (2000 rpm, 10 min) twice. Five microliters of RNase (100 $\mu\text{g/mL}$, Ribonuclease A, Sigma Aldrich, Saint Louis, MO, USA) were added to each tube and incubated for 30 min at 37°C . Next, 50 μL of a 50 $\mu\text{g/mL}$ solution of propidium iodide (PI, 1.0 mg/mL solution in water, Thermo Fisher, Waltham, MA, USA) were added and incubated for 30 min in darkness at room temperature. After incubation, the cells were analyzed using a flow cytometer (FACS Fortessa, Becton Dickinson, Franklin Lakes, NJ, USA). The results were processed using the FACSDiva Version 8.0.2 software (Franklin Lakes, NJ, USA).

2.9. Type of Cell Death

L929 cells were seeded onto sterile 12-well plates at a density of 1×10^4 cells/mL and incubated. After 24 h, when the culture reached 60% confluence, the culture medium was replaced with extracts of the thin film material and incubated over the next 24 h. After incubation, the cells were collected with trypsin, centrifuged (1200 rpm, 8 min, 20°C), and rinsed with PBS twice. The resulting cell pellet was resuspended and washed in a buffer containing calcium ions enabling the binding of annexin V (AV) to phosphatidylserine (PS) (FITC Annexin V Apoptosis Detection Kit, BD Biosciences, Franklin Lakes, NJ, USA) $10\times$ V buffer: 0.1 M HEPES/NaOH pH 7.4, 1.4 M NaCl, 25 mM CaCl_2 , BD Biosciences, Franklin Lakes, NJ, USA). After centrifugation, the supernatant was removed and a solution consisting of 1 μL of annexin V and 30 μL of CaCl_2 buffer was added. The cells were incubated for 15 min in darkness at room temperature. Then, 370 μL of CaCl_2 buffer and 5 μL of propidium iodide were added to the cell suspension. Immediately after staining, analysis was performed using a flow cytometer (FACS Fortessa, Becton Dickinson, Franklin Lakes, NJ, USA). The results were processed using the FACSDiva Version 8.0.2 software (Becton Dickinson, Franklin Lakes, NJ, USA).

2.10. Statistical Analysis

All quantitative data for the statistical analysis originated from at least three independent experiments. The results are shown as mean \pm SD. As a control, the L929 cell line was considered as 100% survival of the L929 cell line. Differences between the groups were considered statistically significant at $p < 0.05$. The effect of incubation time, material type, and extract concentration on cell survival was included in the analysis. Variance was analyzed in a monovalent model for the extracts incubated for 24 and 240 h. To determine the significance of the parameters and the correlations, a post hoc comparison was made using the Bonferroni test. The analysis was performed using the SPSS software (version v20, IBM, New York, NY, USA).

3. Results

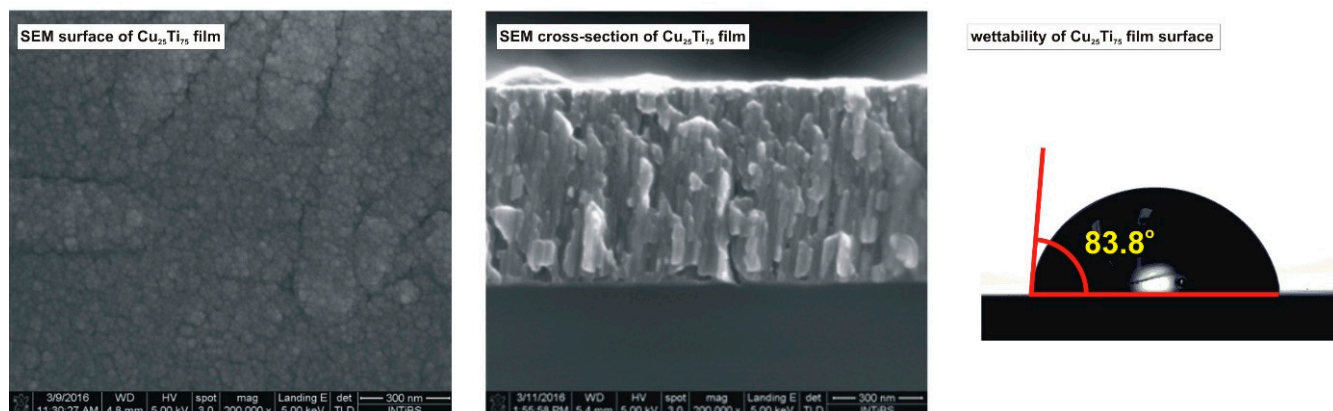
3.1. Physicochemical Properties of Thin Films Based on Cu and Ti

The properties of Cu–Ti films play an important role in contact with living organisms. For this reason, the structure and degree of the oxidation of the elements on the surface were examined and summarized along with the other physicochemical data in Table 1 and Figure 1. The prepared film was nanocrystalline and built from crystallites of the Cu_3Ti_4 phase with an average size of 9.9 nm [18]. The surface of the coating was oxidized, which had a crucial effect on its biological activity. The underlying mechanism was the dominating presence of $\text{Cu}^{0,1+}$ ions and the stabilization of the environment due to the self-passivation of titanium, as confirmed by the predominant share of Ti^{4+} ions on the surface of the coating [18].

Scanning electron microscopy (SEM) showed that the structure and topography of the coating surface was characterized by a high homogeneity of the longitudinal grains, not exceeding approx. 100 nm in length, without empty spaces between the densely packed grains. The hydrophilic nature of the surface promotes cell adhesion [15,18].

Table 1. Physicochemical properties of a nanocrystalline $\text{Cu}_{25}\text{Ti}_{75}$ thin film [15].

Crystal Phase		Cu_3Ti_4
Size of crystallites-D (nm)		9.9
Percentage of copper ions on the surface (%)	$\text{Cu}^{0,1+}$	58.2
	Cu^{2+}	41.8
Amount of copper ions released ((ppb/ mm^2) per day)		0.003

**Figure 1.** SEM (scanning electron microscopy) images of the surface and cross-section of $\text{Cu}_{25}\text{Ti}_{75}$ thin film with the result of wettability measurements—a view of a water drop on the film surface.

3.2. Morphological Evaluation of L929 Fibroblasts in Contact with a Nanocrystalline $\text{Cu}_{25}\text{Ti}_{75}$ Thin Film

The exposure of L929 cells to the $\text{Cu}_{25}\text{Ti}_{75}$ thin film extracts, through both direct and indirect contact, revealed a larger density of the cell monolayer compared to the control. Cell proliferation was inhibited in contact with the thin film extract, but no cytotoxic effect was observed. No abnormalities in cell morphology were noticed in the zone with the highest migration of ions from the thin films, close to the edge of the sample (Figures 2 and 3).

L929 cells in contact with material extracts as well as in direct contact with the sample maintained the correct morphology (no cell lysis and no reduction of cell growth). In direct contact with the sample, no zone of strong migration of copper ions at the edge of the sample was observed (Figure 1).

The size and granularity of the cells after contact with the 100% extract of the $\text{Cu}_{25}\text{Ti}_{75}$ material were comparable to the results of control samples.

A homogeneous population consisted of cells of similar size and granularity. Live cells, characterized by their small size (ca. 100 forward scatter, FSC) and small granularity (ca. 150 side scatter, SSC), were observed (supplementary materials, Figure S1).

3.3. Metabolic Activity

The $\text{Cu}_{25}\text{Ti}_{75}$ thin film extract did not cause a cytotoxic effect on L929 fibroblasts, even after 72 h of incubation with a 100% material extract (Figure 4).

To verify the effect of exposure time and concentration of the $\text{Cu}_{25}\text{Ti}_{75}$ thin film extract, the variance was analyzed in a monovalent model for the extracts incubated for 24 and 240 h. Analysis of variance with repeatable measurements was performed according to the mixed scheme of plan 3 (time of exposure: 24, 48 and 72 h) versus plan 4 (extract concentration: control, 12.5%, 25%, 50%, 100%). Incubation time was the factor measured inside the group, and extract concentration was the factor measured between the samples.

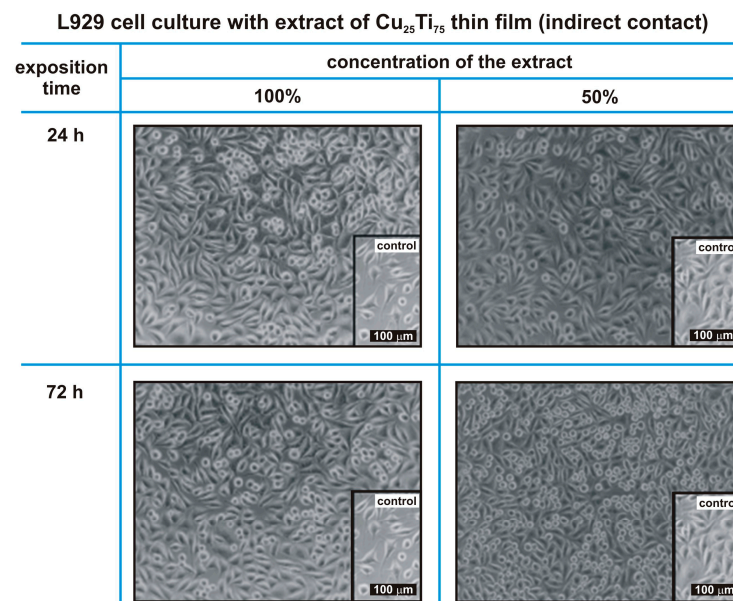


Figure 2. Confluency levels and changes in the morphology of L929 cells in indirect contact (100% and 50% extracts) with Cu₂₅Ti₇₅ thin films, recorded after 24 and 72 h of incubation.

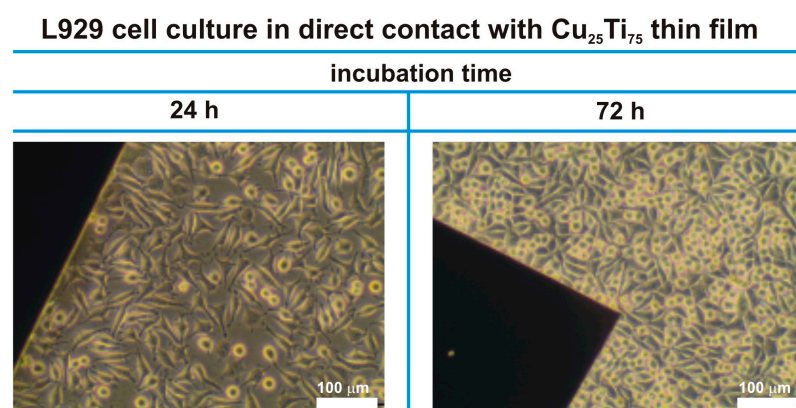


Figure 3. Confluency levels and changes in the morphology of L929 cells in direct contact with Cu₂₅Ti₇₅ thin film, recorded after 24 and 72 h of incubation.

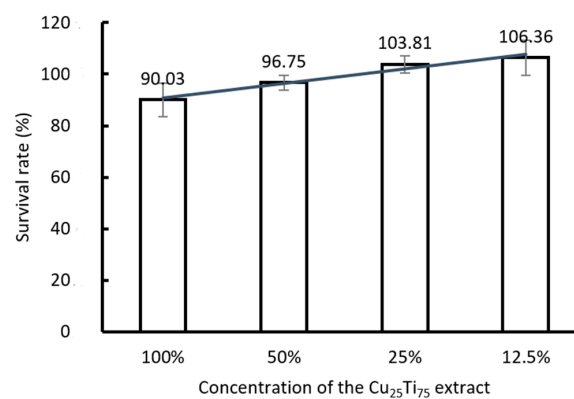


Figure 4. Mitochondrial activity of surviving L929 cells in contact with a 10-day Cu₂₅Ti₇₅ thin film extract (72 h exposure, various extract concentrations, $n = 12$, MTT (3-[4,5-dimethylthiazol-2-yl]-2,5-diphenyl bromide) test), the results are presented in relation to the control (100% activity of unexposed cells).

The most important observation was the effect of exposure time (up to 10 days), which revealed that a longer incubation time significantly increased the differences between the concentrations. Moreover, the higher the extract concentration, the fewer living cells were recorded. For the tested exposure periods, the differences were statistically significant ($p < 0.05$). A high level of accuracy and reliability of the data analysis was confirmed with a standard error value of 0.0081. Detailed statistical data analysis is provided in the supplementary materials.

3.4. L929 Fibroblasts Proliferate When Exposed to $\text{Cu}_{25}\text{Ti}_{75}$ Thin Films

The ability of L929 cells to proliferate when exposed to various concentrations of extracts from a $\text{Cu}_{25}\text{Ti}_{75}$ thin film, as determined with a clonogenic assay, revealed that more colonies had formed than in the unexposed control. This proved the stimulating effect of the $\text{Cu}_{25}\text{Ti}_{75}$ thin film on L929 cell proliferation (Figure 5).

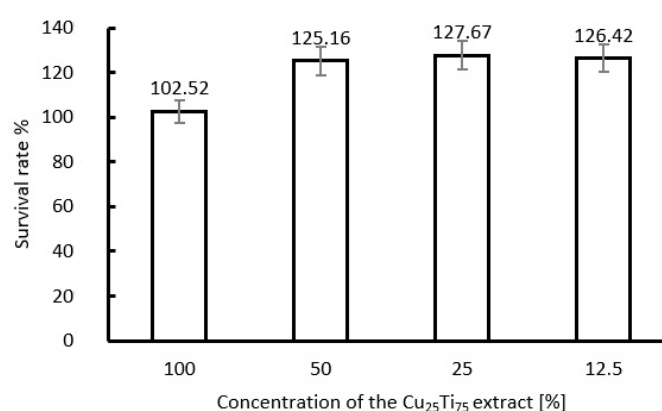


Figure 5. Proliferation of L929 cells exposed to various concentrations of the $\text{Cu}_{25}\text{Ti}_{75}$ extract (8-day exposure, $n = 3$, clonogenic test), the results are presented in relation to the control (100%).

3.5. In Vitro Scarring Test

The rate of migration of L929 cells in the presence of the extracts from the $\text{Cu}_{25}\text{Ti}_{75}$ material was faster compared to the unexposed control and reached 100% of the initial confluence after only six hours of incubation (Figure 6).

It was found that in the case of L929 cells incubated in the control (reference) sample, the analyzed area was covered by cells at the rate of about 10% per hour in relation to its initial size, and the dynamics of this process were close to linear. On the other hand, in the case of the $\text{Cu}_{25}\text{Ti}_{75}$ film, the dynamics of this process were much higher and had a course that can be considered exponential, i.e., after 2 h the analyzed area decreased by 20%, and after 4 h it was 60% lower than the initial state.

3.6. Cell Cycle Phase and Type of Cell Death (Cytometric Test)

Three populations of cells in different phases of the cell cycle were revealed on DNA histograms (Figure 7). Most cells were in the G1 phase, with a higher count for the Cu–Ti extract-exposed cells and a lower count for the proliferative S phase (6.4% and 2.0%, respectively, in relation to the unexposed cells). The survival rate (live vs. dead cells) was higher by 4.4% in relation to the unexposed cells.

The type of cell death was determined after 24 and 48 h of incubation with the $\text{Cu}_{25}\text{Ti}_{75}$ extract. The population of living cells constituted ca. 95% of the total culture. The percentage of cells in contact with the 100% extract of $\text{Cu}_{25}\text{Ti}_{75}$ that bound annexin V was comparable to the control. Notably, a longer exposure to the $\text{Cu}_{25}\text{Ti}_{75}$ extract (24 versus 48 h) decreased the number of viable cells by only 1%.

Based on two-parameter charts, four subpopulations were determined: the populations of necrotic (Q1), early apoptotic, late apoptotic, and living (Q3) cells (Figure 8).

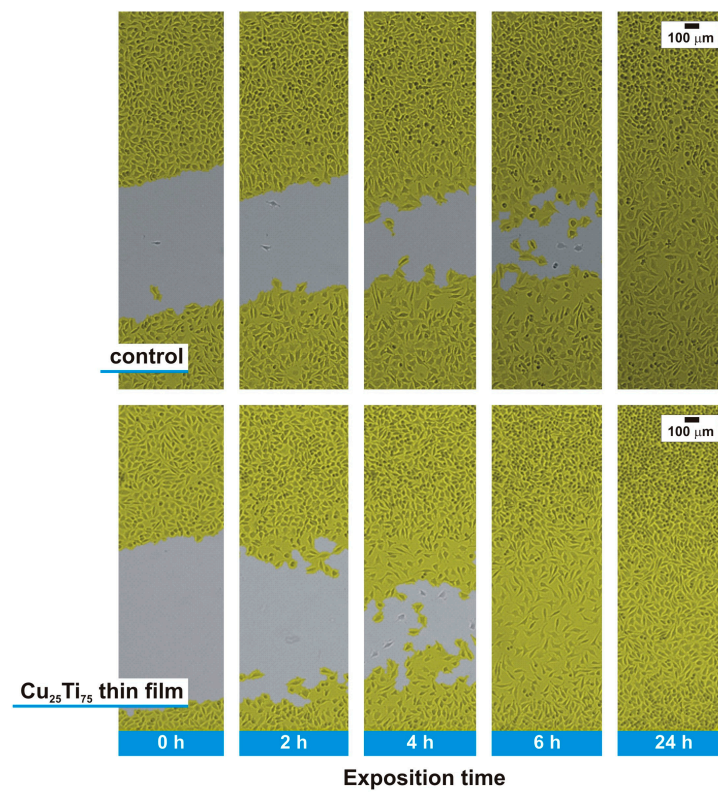


Figure 6. Dynamics of the migration of L929 cells exposed to $\text{Cu}_{25}\text{Ti}_{75}$ thin film extracts, compared to an unexposed control. 24 h incubation, microscopic images, 100 \times magnification.

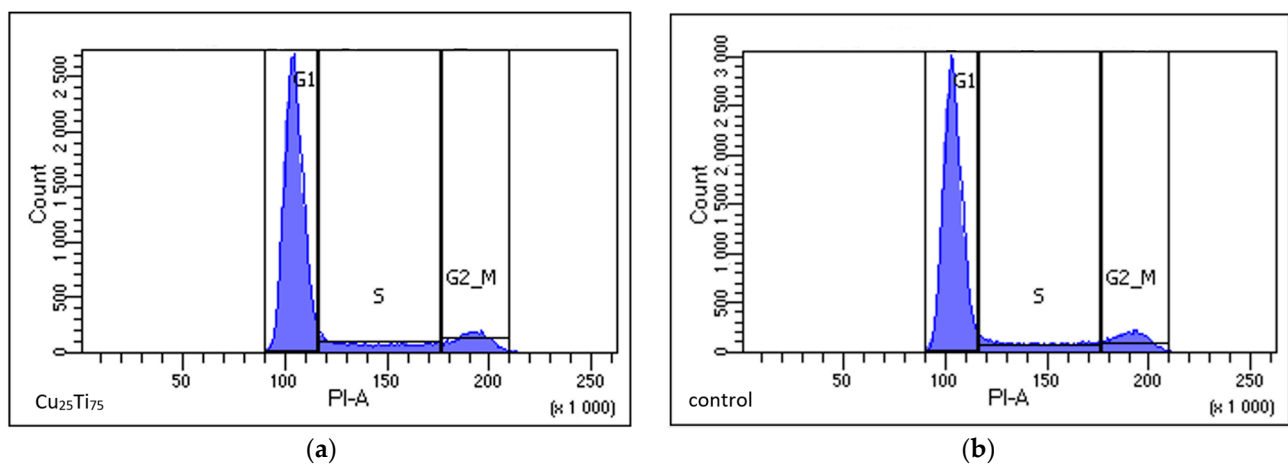


Figure 7. Distribution of Balb/C cells in the cell cycle phase: (a) cells exposed to the $\text{Cu}_{25}\text{Ti}_{75}$ film extract, (b) unexposed cells (control).

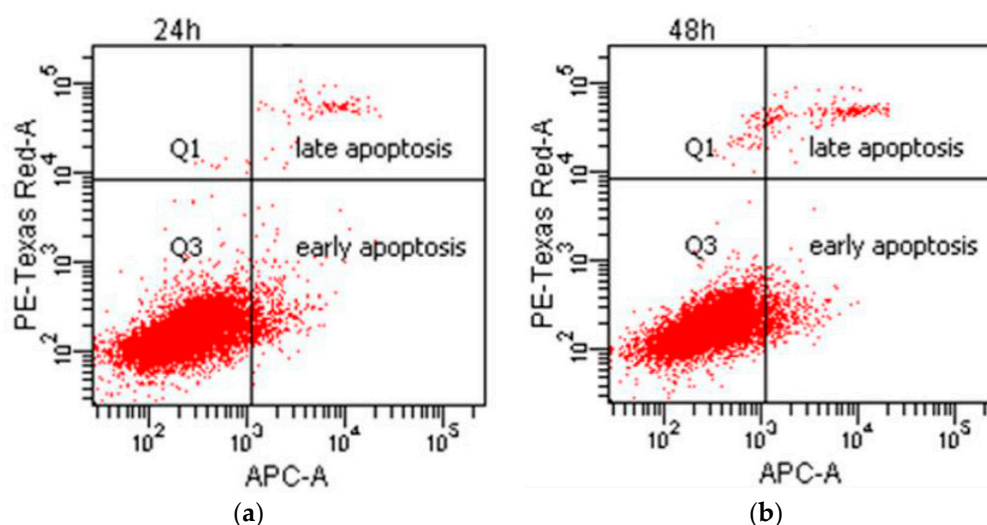


Figure 8. Type of cell death of L929 cells exposed to $\text{Cu}_{25}\text{Ti}_{75}$ extract. Dot plot charts represent the L929 cells after incubation with a 100% $\text{Cu}_{25}\text{Ti}_{75}$ extract after (a) 24 h and (b) 48 h of exposure. Q1—necrotic cells, Q3—living cells.

4. Discussion

This study presented a detailed insight into the biological effects of a nanocrystalline thin film based on copper and titanium on eukaryotic cells in vitro using a mouse fibroblast model.

Copper ions contribute to the proper functioning of the mitochondria and influence cell growth or death depending on the concentration and exposure time. Lüthen et al. [19] indicated the amount of copper ions that caused an increase in cell proliferation (less than 0.3 mmol/L), while a higher dose (0.5 mmol/L) limited growth significantly. Copper is a cofactor of many key enzymes. It is also an indispensable element for the synthesis of about 30 proteins [20–23]. The beneficial effects of copper on tissue regeneration were confirmed over 20 years ago [24], and its impact on all stages of wound healing, e.g., hemostasis, inflammation, proliferation and remodeling, is significant [25,26]. Copper is also responsible for proper cross-linkage in collagen and elastin and is involved in the synthesis of melanin [24,27,28].

Based on our results concerning the thin film variants with different copper and titanium concentrations [15], the optimal relationship between cell survival rate and the amount of copper in the material composition was 25% Cu and 75% Ti. The more copper in the thin film composition, the stronger the cytotoxic effect on L929 cells that was observed [15,29].

Dominance of titanium in the $\text{Cu}_{25}\text{Ti}_{75}$ thin film composition was responsible for the increased self-absorption. Due to the titanium cover, the copper ions migrating from the thin film constituted only 0.5% of the total migration in a single-component copper material [15]. Apparently, titanium provided a protective shield, allowing the copper ions to migrate under controlled conditions.

The results of our previous study [15] have shown that the migration effect of copper ions into their surroundings occurs. In the case of the examined $\text{Cu}_{25}\text{Ti}_{75}$ thin film, the quantity of ions released into the environment during the day was only 0.003 ppb/mm². It is 0.5% of the amount of ions released from the highly cytotoxic Cu coatings. This suggests that 25 at.% of copper content in Cu–Ti film is sufficient to obtain the Ti self-passivation effect, which limits the migration of copper ions to the environment and allows for the stimulation of cell growth. However, for nanocrystalline Cu film, the amount of released ions was 0.616 ppb/mm², which was similar to the $\text{Cu}_{83}\text{Ti}_{17}$ coating where the obtained level was 0.591 ppb/mm². Such migration rate is sufficient to obtain a strong cytotoxic effect. Reduction of the copper content in Cu–Ti film down to 53 at.% resulted in a decrease in the ion migration rate to 0.051 ppb/mm², which resulted in a lack of cytotoxicity (in the

indirect contact). Similar conclusions were drawn by Heidenau et al. [30]. They proved that a proper amount of copper ions has the best effects in achieving a compromise between the bactericidal and non-cytotoxic properties of L929 cells.

The experiments assessing the effect of the Cu–Ti thin film confirmed the high activity of cells after exposure to a 100% Cu₂₅Ti₇₅ extract (Figure 4).

Thin film materials promoting fibroblast proliferation are a promising tool that can be used to protect and support wound regeneration. We have positively verified the effect of a nanocrystalline thin film based on Cu–Ti on in vitro wound healing through stop-motion microscopy. Interestingly, in direct contact with the Cu–Ti thin film, the correct monolayer of mouse fibroblasts was already observed after 24 h of incubation (Figure 1). Similar effects with wound healing in vitro with mesenchymal stem cells were shown by Chen et al. [31], who indicated the effect of copper (in a concentration of 50 µM Cu) on the motility of rat bone marrow stem cells (BMSC). Notably, the promising results obtained by Jeney et al. [32] concerning the effect of copper on wound regeneration in vivo appear to be a good justification for clinical trials; furthermore, in an in vivo study on bone tissue regeneration, a copper-doped material (0.5%, 1% by weight) stimulated the process of angiogenesis and osteosynthesis [32].

The stimulatory effect of copper on cell proliferation has been proven by many researchers [30,33,34]. Our study has also demonstrated such an effect on cell proliferation, and the number of colonies that formed was higher compared to the control (Figure 4). The cell colony growth (assessed using a clonogenic test) was enhanced by exposure to Cu₂₅Ti₇₅ compared to exposure to neutral titanium [15].

No negative effects of the Cu₂₅Ti₇₅ thin film on L929 cell morphology were observed using flow cytometry, i.e., no increased number of cell granules as a response to cellular stress (Figure S1), disturbance in cell cycle phases (Figure 7), or induction of cell death (Figure 8). Altogether, the results indicate no abnormalities in the cells after contact with the Cu₂₅Ti₇₅ extract.

Copper is an essential element responsible for several key processes inside the cell. Homeostasis of the human body (adult, ca. 70 kg weight) requires about 18.86 ppb of copper per day. Consequently, for a full assessment of the biological activity of the thin layer of Cu–Ti (Cu₂₅Ti₇₅), the number of ions released from the material to the environment had to be determined. A minimal migration of copper ions (0.003 ppb/mm²) from the surface was recorded using Atomic absorption spectroscopy (AAS) (Table 1), which did not represent a cytotoxic hazard compared to the daily requirement for this element. As we reported earlier, the release of 0.003 ppb/mm² of Cu caused no toxic effects in mouse fibroblasts, preserving the antimicrobial properties as expected [13,15,16,35].

The degree of ion oxidation determines Cu bioactivity [12,13,36]. Notably, in the Cu₂₅Ti₇₅ thin film, a majority of Cu ions persist in a +1 oxidation state [15]. The level of copper oxidation on the material surface, as well as the quantity of copper ions, contribute strongly to the antimicrobial effect, representing a crucial factor for the possible biological applications of this type of nanocrystalline Cu–Ti material [15].

In the case of the examined Cu₂₅Ti₇₅ thin film, the effect of bonding copper atoms with titanium prevents the migration process. This has a key impact on reducing cytotoxicity and obtaining the effect of stimulating cell growth.

5. Conclusions

This study showed a unique effect of a Cu₂₅Ti₇₅ thin film on mouse fibroblast cells. The results concerning mitochondrial activity, cell proliferation, and migration proved that the material is nontoxic and has proliferative properties that indicate the stimulating effect of the Cu₂₅Ti₇₅ thin film on the cells. Such characteristics of the nanocrystalline Cu–Ti thin film are highly promising for further research towards the development of new multifunctional biomaterials.

Supplementary Materials: The following are available online at <https://www.mdpi.com/2079-6412/11/3/300/s1>, Figure S1: Morphological evaluation of L929 murine fibroblasts after exposure to extracts from the Cu₂₅Ti₇₅ thin film (a and b), and control (c and d); the test was performed after 24 and 48 h of incubation, respectively.

Author Contributions: Conceptualization, M.O. and D.W.; methodology, M.O. and D.W.; investigation, M.O., M.M., and D.W.; writing—original draft preparation, M.O. and B.S.; writing—review and editing, D.W. and D.K.; visualization, M.M. and A.O.; supervision, D.K. All authors have read and agreed to the published version of the manuscript.

Funding: This study was financed by the Polish National Science Centre (NCN), research project No. UMO-2016-21-B-ST8-02099.

Institutional Review Board Statement: Not applicable.

Informed Consent Statement: Not applicable.

Data Availability Statement: The data presented in this study are available in this article and supplementary material.

Conflicts of Interest: The authors declare no conflict of interest.

References

- Murr, L.E. Strategies for creating living, additively manufactured, open-cellular metal and alloy implants by promoting osseointegration, osteoinduction and vascularization: An overview. *J. Mater. Sci. Technol.* **2019**, *35*, 231–241. [\[CrossRef\]](#)
- Kohn, D.H. Porous coatings in orthopedics. In *Comprehensive Biomaterials*; Ducheyne, P., Ed.; Elsevier Science: Amsterdam, The Netherlands, 2011. [\[CrossRef\]](#)
- Wilson, J. Metallic biomaterials: State of the art and new challenges. In *Fundamental Biomaterials: Metals*; Balakrishnan, P., Ed.; Woodhead Publishing Series in Biomaterials; Woodhead Publishing: Shaston, UK, 2018; pp. 1–33. [\[CrossRef\]](#)
- Kaur, M.; Singh, K. Review on titanium and titanium based alloys as biomaterials for orthopaedic applications. *Mater. Sci. Eng. C* **2019**, *102*, 844–862. [\[CrossRef\]](#)
- Kikuchi, M.; Takahashi, M.; Okabe, T.; Okuno, O. Grindability of dental cast Ti–Ag and Ti–Cu alloys. *Dent. Mater. J.* **2003**, *22*, 191–205. [\[CrossRef\]](#)
- Takahashi, M.; Kikuchi, M.; Takada, Y.; Okuno, O. Grindability and mechanical properties of experimental Ti–Au, Ti–Ag and Ti–Cu alloys. *Int. Congr. Ser.* **2005**, *1284*, 326–327. [\[CrossRef\]](#)
- Liu, R.; Memarzadeh, K.; Chang, B.; Zhang, Y.; Ma, Z.; Allaker, R.P.; Ren, L.; Yang, K. Antibacterial effect of copper-bearing titanium alloy (Ti–Cu) against *Streptococcus mutans* and *Porphyromonas gingivalis*. *Sci. Rep.* **2016**, *6*, 29985. [\[CrossRef\]](#)
- Mei, S.; Wang, H.; Wang, W.; Tong, L.; Pan, H.; Ruan, C.; Ma, Q.; Liu, M.; Yang, H.; Zhang, L. Antibacterial effects and biocompatibility of titanium surfaces with graded silver incorporation in titania nanotubes. *Biomaterials* **2014**, *35*, 4255–4265. [\[CrossRef\]](#)
- Niinomi, M. Recent metallic materials for biomedical applications. *Metall. Mat. Trans. A* **2002**, *33*, 477–486. [\[CrossRef\]](#)
- Wojcieszak, D.; Mazur, M.; Kaczmarek, D.; Szponar, B.; Grobelny, M.; Kalisz, M.; Pelczarska, A.; Szczygiel, I.; Poniedziałek, A.; Osekowska, M. Structural and surface properties of semitransparent and antibacterial (Cu,Ti,Nb)O_x coating. *Appl. Surf. Sci.* **2016**, *380*, 159–164. [\[CrossRef\]](#)
- Wojcieszak, D.; Mazur, M.; Kaczmarek, D.; Mazur, P.; Szponar, B.; Domaradzki, J.; Kepinski, L. Influence of the surface properties on bactericidal and fungicidal activity of magnetron sputtered Ti–Ag and Nb–Ag thin films. *Mater. Sci. Eng. C* **2016**, *62*, 86–95. [\[CrossRef\]](#) [\[PubMed\]](#)
- Park, Y.J.; Song, Y.H.; An, J.H.; Song, H.J.; Anusavice, K.J. Cytocompatibility of pure metals and experimental binary titanium alloys for implant materials. *J. Dent.* **2013**, *41*, 1251–1258. [\[CrossRef\]](#)
- Shedle, A.; Samorapoompichit, P.; Rausch-Fan, X.H.; Franz, A.; Fureder, W.; Sperr, W.R.; Sperr, W.; Ellinger, A.; Slavicek, R.; Boltz-Nitulescu, G.; et al. Response of L929 fibroblasts, human gingival fibroblasts, and human tissue mast cells to various metal cations. *J. Dent. Res.* **1995**, *74*, 1513–1520. [\[CrossRef\]](#)
- Yamamoto, A.; Honma, R.; Sumita, M. Cytotoxicity evaluation of 43 metal salts using murine fibroblasts and osteoblastic cells. *J. Biomed. Mater. Res.* **1998**, *39*, 331–340. [\[CrossRef\]](#)
- Wojcieszak, D.; Osekowska, M.; Kaczmarek, D.; Szponar, B.; Mazur, M.; Mazur, P.; Obstarczyk, A. Influence of material composition on structure, surface properties and biological activity of nanocrystalline coatings based on Cu and Ti. *Coatings* **2020**, *10*, 343. [\[CrossRef\]](#)
- Wojcieszak, D.; Kaczmarek, D.; Antosiak, A.; Mazur, M.; Rybak, Z.; Rusak, A.; Batycka, M.; Poniedziałek, A.; Domaradzki, J.; Gamian, A.; et al. Antimicrobial activity and impact on living cells of Cu–Ti thin films in relation to their surface properties. *Mater. Sci. Eng. C Mater. Biol. Appl.* **2015**, *56*, 48–56. [\[CrossRef\]](#)
- Wojcieszak, D.; Mazur, M.; Kaczmarek, D.; Poniedziałek, A.; Osekowska, M. An impact of the copper additive on photocatalytic and bactericidal properties of TiO₂ thin films. *Mater. Sci. Pol.* **2017**, *35*, 421–426. [\[CrossRef\]](#)

18. Adamiak, B.; Wiatrowski, A.; Domaradzki, J.; Kaczmarek, D.; Wojcieszak, D.; Mazur, M. Preparation of multicomponent thin films by magnetron co-sputtering method: The Cu–Ti case study. *Vacuum* **2019**, *161*, 419–428. [[CrossRef](#)]
19. Lüthen, F.; Bergemann, C.; Bulnheim, U.; Prinz, C.; Neumann, H.; Podbielski, A.; Bader, R.; Rychly, J. A dual role of copper on the surface of bone implants. *Mater. Sci. Forum* **2010**, *638–642*, 600–605. [[CrossRef](#)]
20. Banci, L.; Bertini, I.; Cantini, F.; Ciofi-Baffoni, S. Cellular copper distribution: A mechanistic systems biology approach. *Cell. Mol. Life Sci.* **2010**, *67*, 2563–2589. [[CrossRef](#)]
21. Prohaska, J.R.; Heller, L.J. Mechanical properties of the copper-deficient rat heart. *J. Nutr.* **1982**, *112*, 2142–2150. [[CrossRef](#)]
22. Arredondo, M.; González, M.; Olivares, M.; Pizarro, F.; Araya, M. Ceruloplasmin, an indicator of copper status. *Biol. Trace Elem. Res.* **2008**, *123*, 261–269. [[CrossRef](#)]
23. Chambers, A.; Krewski, D.; Birkett, N.; Plunkett, L.; Hertzberg, R.; Danzeisen, R.; Aggett, P.J.; Starr, T.B.; Baker, S.; Dourson, M.; et al. An exposure-response curve for copper excess and deficiency. *J. Toxicol. Environ. Health B Crit. Rev.* **2010**, *13*, 546–578. [[CrossRef](#)]
24. Huffman, D.L.; O'Halloran, T.V. Function, structure, and mechanism of intracellular copper trafficking proteins. *Annu. Rev. Biochem.* **2001**, *70*, 677–701. [[CrossRef](#)] [[PubMed](#)]
25. Failla, M.L. Roles of trace metals in the maturation, activation and effector functions of immune cells. *Bibl. Nutr. Dieta.* **1998**, *54*, 103–111. [[CrossRef](#)]
26. Sen, C.K.; Khanna, S.; Venojarvi, M.; Trikha, P.; Ellison, E.C.; Hunt, T.K.; Roy, S. Copper-induced vascular endothelial growth factor expression and wound healing. *Am. J. Physiol. Heart Circ. Physiol.* **2002**, *282*, H1821–H1827. [[CrossRef](#)] [[PubMed](#)]
27. Harris, E.D. Basic and clinical aspects of copper. *Crit. Rev. Clin. Lab. Sci.* **2003**, *40*, 547–586. [[CrossRef](#)] [[PubMed](#)]
28. Kobayashi, H.; Ishii, M.; Chanoki, M.; Yashiro, N.; Fushida, H.; Fukai, K.; Kono, T.; Hamada, T.; Wakasaki, H.; Ooshima, A. Immunohistochemical localization of lysyl oxidase in normal human skin. *Br. J. Dermatol.* **1994**, *131*, 325–330. [[CrossRef](#)]
29. Liu, Y.; Tay, J.-H. Detachment forces and their influence on the structure and metabolic behaviour of biofilms. *World J. Microb. Biot.* **2001**, *17*, 111–117. [[CrossRef](#)]
30. Heidenau, F.; Mittelmeier, W.; Detsch, R.; Haenle, M.; Stenzel, F.; Ziegler, G.; Gollwitzer, H. A novel antibacterial titania coating: Metal ion toxicity and in vitro surface colonization. *J. Mater. Sci. Mater. Med.* **2005**, *16*, 883–888. [[CrossRef](#)]
31. Chen, X.; Hu, J.G.; Huang, Y.Z.; Li, S.; Li, S.F.; Wang, M.; Xia, H.W.; Li-Ling, J.; Xie, H.Q. Copper promotes the migration of bone marrow mesenchymal stem cells via Rnd3-dependent cytoskeleton remodeling. *J. Cell Physiol.* **2020**, *235*, 221–231. [[CrossRef](#)]
32. Jeney, F.; Bazsó-Dombi, E.; Oravecz, K.; Szabó, J.; Nagy, I.Z. Cytochemical studies on the fibroblast-preadipocyte relationships in cultured fibroblast cell lines. *Acta Histochem.* **2000**, *102*, 381–389. [[CrossRef](#)]
33. Yu, L.; Jin, G.; Ouyang, L.; Wang, D.; Qiao, Y.; Liu, X. Antibacterial activity, osteogenic and angiogenic behaviors of copper-bearing titanium synthesized by PIII&D. *J. Mater. Chem. B* **2016**, *4*, 1296–1309. [[CrossRef](#)] [[PubMed](#)]
34. Zheng, K.; Dai, X.; Lu, M.; Hüser, N.; Taccardi, N.; Boccaccini, A.R. Synthesis of copper-containing bioactive glass nanoparticles using a modified Stöber method for biomedical applications. *Colloids Surf. B Biointerfaces.* **2017**, *150*, 159–167. [[CrossRef](#)] [[PubMed](#)]
35. Ma, Z.X.; Ren, L.; Liu, R.; Yang, K.; Zhang, Y.; Liao, Z.; Liu, W.; Qi, M.H.; Misra, R.D. Effect of heat treatment on Cu distribution, antibacterial performance and cytotoxicity of Ti–6Al–4V–5Cu alloy. *J. Mater. Sci. Technol.* **2015**, *31*, 723–732. [[CrossRef](#)]
36. Saphier, M.; Silberstein, E.; Shotland, Y.; Popov, S.; Saphier, O. Prevalence of monovalent copper over divalent in killing *Escherichia coli* and *Staphylococcus aureus*. *Curr. Microbiol.* **2018**, *75*, 426–430. [[CrossRef](#)] [[PubMed](#)]